A Novel 3D pillar-layered Metal-Organic Framework: Pore-size-dependent Catalytic activity and CO_2/N_2 affinity

Hosein Ghasempour,[a] Alireza Azhdari Tehrani,[a] Ali Morsali,[*a] Jun Wang,[b] and Peter C. Junk[b]

[a] Department of Chemistry, Faculty of Sciences, Tarbiat Modares University, P.O. Box 14115-175, Tehran, Iran

[b] College of Science Technology and Engineering, James Cook University, Townsville Qld, 4811, Australia

Abstract

The structure-activity relationship plays the main role in the applicability of Metal-organic Frameworks (MOFs) in different areas including catalysis. Regarding to this herein a novel pillar-layered MOF (TMU-52) that is isostructural to our recently reported TMU-25 is introduced. The structure of this framework was analyzed using X-ray crystallography, FT-IR spectroscopy, Thermogravimetric and elemental analyses. According to the similar organic and inorganic backbone, a comparative study was done on catalytic manner of TMU-25 and TMU-52 toward in aldol-type condensation reaction. TMU-52 was designed through replacing the biphenyl core in the pillar linker of TMU-25 with phenyl group as a better candidate heterogeneous catalysis. The selectivity of the TMU-52 was higher owing to its narrower channels. CO_2/N_2 affinity of these structures was also investigated.

Keywords: Coordination polymers, Metal organic Frameworks; catalysis; Functional materials; aldol-type reaction; X-ray crystallography.

Introduction

Metal-organic Frameworks (MOFs) are new supreme class of crystalline materials with unique properties such as high porosity, low density, topological diversity and tunability [1, 2]. These materials have extremely attractive in areas as heterogeneous catalysis [3], gas storage [4], separation [5], pollutants removal [6] and so on [7]. Among different type of MOFs, pillar-layered

metal-organic frameworks [8] are widely studied due to their simple fabrication and structural diversity, [9]. Pillar-layered MOFs have highly designable nature because in addition to metal sites and O-donor linkers, there is one more possibility for functionality and diversity as N-donor pillaring linker [10]. This organic linker moieties can be simply modified and subsequently, through little change in its backbones the pore environment can be rationally designed and optimized for desired applications [11]. The existence of two bridging ligands with possibility of carrying basic functionalities make pillar-layered MOFs promising candidates for heterogeneous catalysis [12]. One important reaction to be studied in organic synthesis is Carbon−Carbon Double Bond Formation which is commonly applied in biological and pharmaceutical targets [13]. Michael additions and Diels−Alder reactions are two most general examples of this reaction types producing useful multi-substituted alkenes [14]. Although the homogenous catalysts are broadly used in this type of reactions, the recyclability, stability and high recovery cost are remaining challenges. Hence, developing heterogeneous catalysts with high stability and good recyclability is mostly desired [15]. Among reported porous materials, MOFs provide suitable platform as heterogeneous catalyst owing to their accessible pores and functional groups. Among different MOF subclasses, pillar-layered MOFs with basic functional groups can be a promising candidates as heterogeneous catalysis [16]. Specifically, it has been indicated that −NH_2 functionalities on ligands improve the basicity of MOF structure and enhance the overall conversion in reactions that require to a basic catalyst [17].

Another remarkable strategy beside functionality, is pore size optimization that has been infrequently reported for pore-size-dependent selective catalysis [18]. Applying this strategy in our previous work [12] on four isoreticular metal-organic frameworks (IRMOFs) [19] provide us an opportunity for understanding the exact structure–function relations [20]. In consequence of their structural resemblance, a systematically study on the effects of pillar linkers with different length on MOF's aperture size was done. Hence using this strategy, here we report synthesis, characterization and investigation of catalytic behavior of a new pillar-layered MOF, [Zn(L1)(NH_2-bdc)].0.5DMF (TMU-52) [NH_2-bdc: 2-aminoterephethalic acid, L1: N4,N4'-bis(pyridin-4-ylmethylene)-phenyl-4,4'-diamine, DMF: Dimethylformamide] which is isoreticular to our recently reported [Zn(NH_2-bdc)(L2)].2DMF (TMU-25) [L2: N4,N4'-bis(pyridin-4-ylmethylene)-biphenyl-4,4'-diamine] [21]. Both of these frameworks possess free −NH_2, imine groups and narrow channels which made them potential candidates for competitive size-selective

catalytic study. So, aldol-type condensation reaction was developed with these isoreticular MOF catalysts.

On the other hand, the functional pillar-layered MOFs with highly ordered pores also show great potential for separation and selective gas adsorption [22],[23]. Accordingly, selective CO_2 adsorption over N_2 behaviour of TMU-52 and TMU-25 was investigated. The $-NH_2$ functionality of pillars improve the CO_2 adsorption via formation of H-bonds. Interestingly, the observed results of gas adsorption were confirmed by the catalytic selectivity of structures.
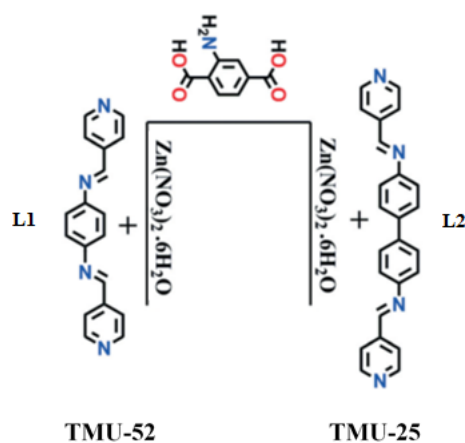

Scheme 1. Chemical structure of NH_2-bdc and auxiliary ligand, namely L2 and L1 in TMU-25 and TMU-52.

Results and Discussion

TMU-52 was fabricated by solvothermal reaction of $Zn(NO_3)_2.6H_2O$, NH_2-bdc and L1 ligands at 90˚C for three days to give light brown appropriate X-ray quality crystals (scheme1).

Single crystal X-ray diffraction revealed that TMU-52 crystallized in the Triclinic P^{-1} space group. There are some reported structures using L1 ligand as a pillaring ligand like TMU-6 and TMU-35 frameworks. [24, 25]. TMU-6 was containing bent 4,4-Oxybisbenzoic acid (OBA) dicarboxylic ligand resulted three-fold interpenetrated structure. In TMU-35 coordinating the bent urea based dicarboxylic acid ligand to Zn forming binuclear paddle-wheel secondary building unit (SBUs) which were connected from axial sits by L1 ligand to form quadruply interpenetrated 3D pillared-

layer framework. Using linear NH_2-bdc dicarboxylic acid instead of bent dicarboxylic ligand lead to two-fold interpenetrated TMU-52. In the binuclear SBU of TMU-52 (Zn···Zn separation is 3.852(1) Å) two neighbouring penta-coordinated metal nodes adopt similar distorted octahedral coordination geometry, with three sites coordinated by oxygen atoms from three different carboxylate groups of NH_2-bdc ligand to form two-dimensional (2D) layers and the axial sites are coordinated to nitrogen atoms from two pyridyl rings of L1 ligands, which act as pillars to link 2D layers to form a pillared 3D network (Fig.1 and Fig. S3). Topological analysis by TOPOS program suggests the overall 3D structure of TMU-52 has pcu(α-Po) topology with Schläfli symbol of $\{4^{12}.6^3\}$ [26].
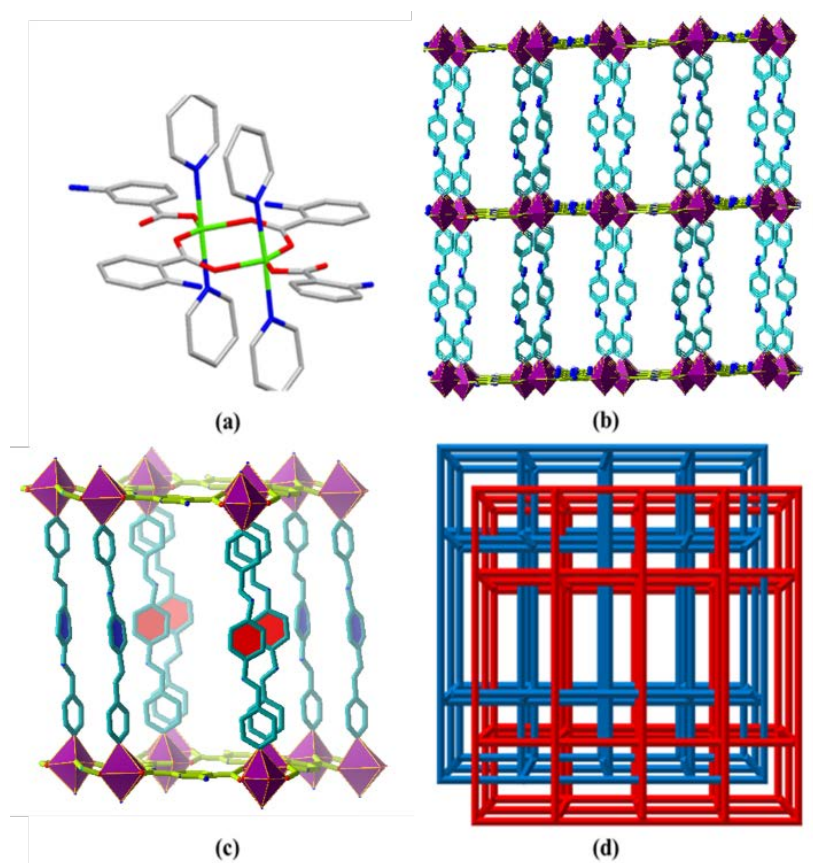
Figure 1. Crystal structure illustration of TMU-52: (a) Binuclear secondary building units, (Zn: green; O: red; N: blue; C: gray). (b) Wires or sticks model demonstrating of 3D framework of TMU-52 along *a* axis. (c) Parallel orientation of L1 ligands in TMU-52, and (d) Schematic Simplified overall of two-fold network interpenetration in TMU-52.

The calculated void space, determined using PLATON software [27] for guest- and disorder-free TMU-52 is 31.3% (1898.7 Å3). For calculating the percentage of intermolecular non-covalent contacts in the crystal packing of TMU-25 and TMU-52, Hirshfeld surface analysis was used. Table S1 summarizes the percentage contributions of different intermolecular contacts. The H⋯H interactions have the highest influence to the Hirshfeld surface areas in both of these frameworks (42.6% for TMU-25 and 36.8% for TMU-52). The π-interactions, containing π⋯π stacking and C–H⋯π also show main effect in the Hirshfeld surface areas, while O⋯H and N⋯H hydrogen bonds (14.1% for TMU-25 and 10.7% for TMU-52) have a less significant contribution to the Hirshfeld surface area (Fig. 2).
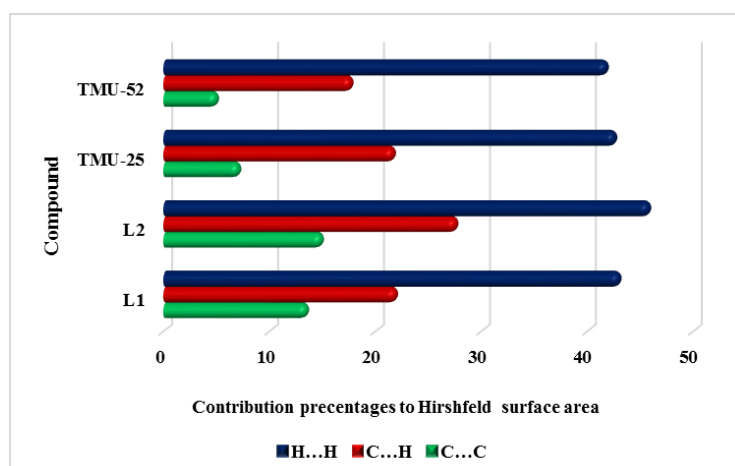
Figure 2. Relative contributions of various non-covalent contacts to the Hirshfeld surface area in compounds L1, L2, TMU-25 and TMU-52.
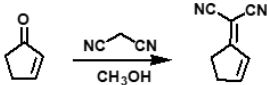
To remove the guest DMF molecules existing in the pores of TMU-52, the prepared compound was immersed in chloroform for 5 days, with fresh chloroform added every 24 hours, filtered and dried at 80 °C under vacuum for at least 24 hours. The activation of this MOF was also confirmed by FT-IR spectroscopy, elemental analysis and powder X-ray diffraction (Fig. S4 and S8).
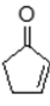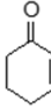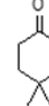
The FT-IR spectra of TMU-25 and TMU-52 materials achieved by the solvothermal method are indistinguishable (Fig. S5). Two peaks at 3470 and 3359 cm^{-1} in FT-IR spectrum of TMU-52 can be related to the amino groups of the NH$_2$-bdc ligand. Also, two strong bands at 1575 and 1385 cm^{-1}, are respectively assigned to the asymmetric and symmetric vibrations of the carboxylate group. The FT-IR spectra of TMU-25 showed the same manner. Also as illustrated in figure S6, adequate similarities were observed between the experimental powder XRD patterns of TMU-25 and TMU-52 that reveal their isoreticularity. Also, comparison between the XRD pattern of methanol treated samples with the as-made crystal patterns indicated that the TMU-25 and TMU-52 MOFs are stable in the catalytic reaction condition (MeOH and 60 ˚C for 24h).

Thermogravimetric analyses (TGA) indicate that TMU-52 has relatively higher thermal stability compared with TMU-25 at elevated temperatures (Fig. S7). As shown in figure S7, The TGA diagram of CH$_3$Cl-exchanged TMUs (exchanged for 5 days) shows the first weight loss before 80℃ which is due to the guest molecules removal. Second step of weight loss probably related to the decomposition step, occurs after 350℃ for TMU-52, while in the TMU-25 case this step is starting in earlier temperature.

Since the backbone structure of TMU-52 and TMU-25 are the same and both of them possess imine and free −NH$_2$ groups, except for the length of their channels that raises from different pillar ligand lengths (L1= 15.6 Å and L2= 19.9 Å), these frameworks may be good cases for comparative catalytic investigation. As previously reported, it was showed that basic amino-functionalized and weak basic imine groups in TMU-25 can catalyze the Knoevenogel reaction at room temperature [28]. The aldol-type coupling reaction of malononitrile with α,β-unsaturated carbonyl compounds was studied in the present work. These α,β-unsaturated ketones have less activity toward nucleophilic attack which make this type of condensation harder to proceed. No detectable product was observed during the reaction of malononitrile and 1-cyclohexen-2-one, even at elevated temperature (60℃, in the absence of catalyst and in MeOH as solvent within 24 h), whereas Knoevenogel reaction of malononitrile and benzaldehyde in the absence of any catalyst produced around 20% of the product at room temperature.

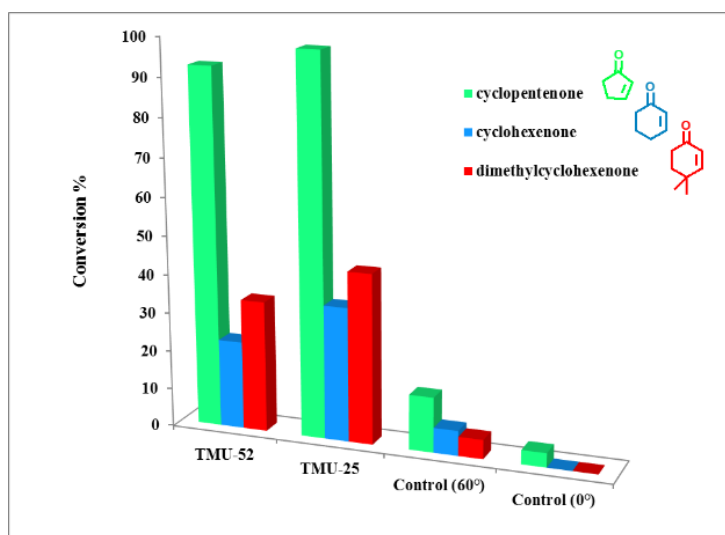**Table 1.** Coupling reaction of malononitrile and carbonyl compounds with the prepared MOFs within 24h.

	Catalyst	Yield (%)[a]	Yield (%)	Yield (%)
1	NH₂-bdc	16.8	6.1	2.8
2	L1	22.7	15	9.5
3	L2	29.4	19.2	8.2
4	TMU-25	**98.7**	36.0	46.1
5	TMU-52	**92.7**	24.3	33.99

[a] GC yield, reaction conditions; substrates (0.2 mmol). Malononitrile (0.3 mmol), catalysts (2 mol%, 10 mg), MeOH (3 ml), 60℃.

At the first step of the catalytic reaction examinations, the polar solvents (methanol, ethanol, acetonitrile) were used to optimize the reaction. Finally, the reaction mixtures proceeded in methanol in the presence of MOFs and progress was analysed with gas chromatography. As a result, during the reaction analysis of substrate 1-cyclohexen-2-one, in the presence of these two solid base MOF catalysts, the results were obtained applying 2 mol% of the catalysts, and in methanol as solvent at 60℃. As summarized in Table 1, after 24 h of reaction results indicate that the catalytic activity of TMU-25 with slightly larger channels and biphenyl pillar core is more than TMU-52 with phenyl core (36.0% and 24.3%, respectively). For exact investigation of the catalysis activity of these two MOFs, 1-cyclopenten-2-one as smaller and 4,4-dimethyl-1-cyclohexen-2-one as larger substrates were added and separately reacted in the presence of the both MOF catalysts in the same reaction conditions. Details specifies that in the case of 4,4-dimethyl-1-cyclohexen-2-one, partly similar results were accomplished in the presence of both TMU-52 and TMU-25 which forms 33.9% and 46.1% of the corresponding addition product, respectively. Interestingly, after 24 hours the reaction of 1-cyclopenten-2-one as smallest substrate with malononitrile, TMU-52 and TMU-25 produced 92.7% and 98.7% of product, respectively. As illustrated in figure 3, the results are a proof of the substrate selectivity for smallest 1-cyclopenten-2-one in both TMUs. The higher rates of reaction of small substrates in comparison to larger ones with TMUs suggest that by 1-cyclopenten-2-one as smallest substrate catalysis primarily occurs within the pores. As was shown clearly in table 2, the catalytic performance of TMUs is dependent on the substrate size. In fact, the narrow channel of these frameworks is the controlling parameter for higher permeation capability of smallest substrate into the pores which led to higher organic
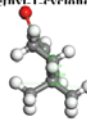
transformation. In another hand, controlling the hydrophobicity character can also affect the catalytic performance of MOF. Higher hydrophobicity reduces the wettability of the pore surfaces to eventually create moisture-stable MOF structures. In this regard, introduction of hydrophobic organic moieties inside the pores of MOFs can be effective tool to achieve better catalysts. Replacement of phenyl core of L1 ligand in TMU-52 by the biphenyl core of L2 in TMU-25 may create a more hydrophobic environment resulting the improvement in the interactions between 4,4-dimethyl-1-cyclohexen-2-one (the biggest substrate) and TMU-25 framework more than TMU-52 framework (46.1% versus 33.9%). Interestingly with applying more reaction time (48 h) the selectivity was more considerable, especially for TMU-52 (Table S2 and Fig. 4). This can be attributed to i) the narrower channels of TMU-52 in comparison to TMU-25 channels, and ii) the more hydrophobic surface of TMU-25 which is more favor for larger substrates. The results indicated that a slight change in around the basic reaction center in MOF structure could interestingly change the preference of the substrates to be reacted while they have very little structure diversity.

Figure 3. Comparison of the catalyst reactivity of TMU-52 and TMU-25 toward various substrates and their control reaction in MeOH at 60 °C within 24h.

Table 2. Catalytic performance of TMU-25/-52 in aldol-type condensation of malononitrile and carbonyl compounds dependent on substrates' size within 24h.

Catalyst	Aperture size	Substrates' size		
		1-cyclopenten-2-one	1-cyclohexen-2-one	4,4-dimethyl-1-cyclohexen-2-one
		4.06×1.86	4.43×2.94	6.5×4.37
		Conversion %[a]		
TMU-25	3.43×14.81	98.7	36.0	46.1
TMU-52	2.92×10.06	92.7	24.3	33.99

[a] GC yield, reaction condition: substrate (0.2 mmol), malononitrile (0.3 mmol), catalysts (2 mol%, 10 mg), MeOH (3 ml), 60 °C.

The product resulted from smallest substrate was surveyed via FT-IR spectroscopy and ^{1}H NMR analysis. The FT-IR data (ESI) revealed that C=O bond was replaced with C=C bond. Also, the nitrile group of products was observed at the absorption bond at 2207 cm^{-1}. Furthermore, the exact structure of the product attained from the smallest substrates determined by ^{1}H NMR, point to formation through a 1,2-addition reaction into the carbonyl compounds followed by a water molecule elimination from the product, instead of 1,4-addition that was also confirmed by the disappearance of the carbonyl group vibration in the FT-IR spectra.

As observed in figure 5, TMU-52 can be recycled and reused for at least five reaction cycles without noticeable loss of its activity, but TMU-25 shows slightly decrease in reactivity, that can be attributed to the its lower thermal stability and loss of crystallinity during reaction cycles.
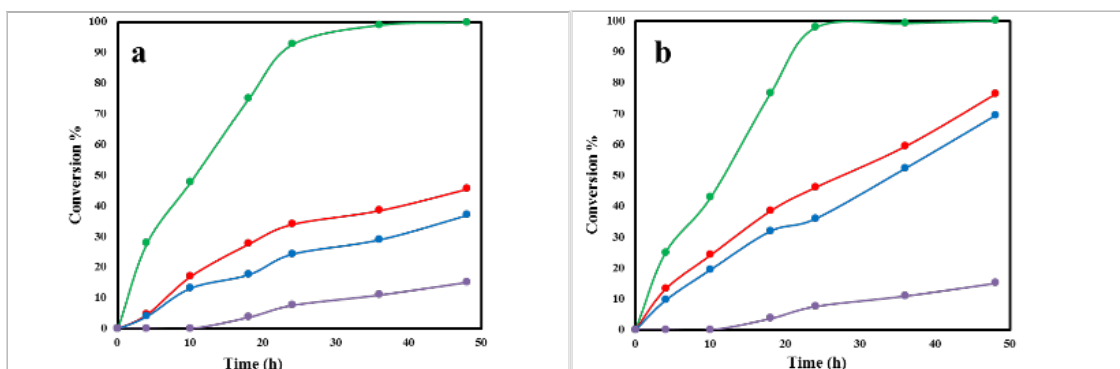
Figure 4. Yield-versus-time profile of aldol-type condensation reaction of 1-cyclopenten-2-one (green), 1-cyclohexen-2-one (blue) and 4,4-dimethyl-1-cyclohexen-2-one (red) catalyzed by TMU-52 (a) and TMU-25 (b), (control reaction with 1-cyclopenten-2-one = violet).

Although the XRD pattern of the used TMU-52 catalyst after the 5th run shows relatively losses crystallinity and some peaks shows broadening in XRD pattern, but the main peaks (2θ= 4.44, 13.40, 17.76) are remained in comparison with the as-synthesis sample pattern (Fig. S8). ICP analysis was performed for investigating the heterogeneity of the catalyst system using the filtrate reaction mixture of 1-cyclopenten-2-one after 24 h. The results demonstrated that less than 0.5% remaining zinc was identified which confirmed that more than 99% of the zinc metal center does not leach into the reaction mixture during the condensation reaction. These data confirming with XRD, reveal that no metal and/or pillar leaching occurred as well no reaction was performed through homogeneous processes.
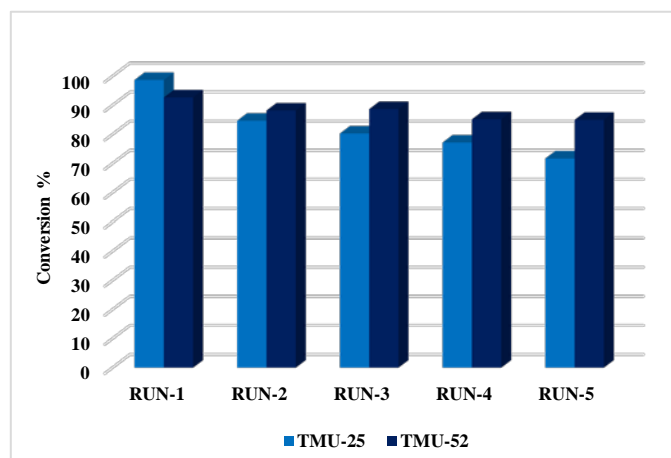
Figure 5. Reusability of TMU-25 (blue) and TMU-52 (Navy blue) in aldol-type condensation reaction of 2-cyclopenten-1-one with malononitrile in MeOH at 60 °C.

The more accessible channel of TMU-25 also was proved by gas adsorption results. Similar to TMU-25, TMU-52 is also non-porous to N_2 at 77 K, but both frameworks are porous to CO_2 at 195 K [84.26 cm^2/g at STP, for TMU-25 and 52.4 cm^2/g at STP, for TMU-52);]. In small pores N_2 cannot enter at 77 K while CO_2 adsorption is taking place at higher temperature (195 K) at which

more thermal and vibrational flexibility of the network for the insertion of even large guest molecules is allowed. The observed CO_2/N_2 porosity of these structures can be regarded to stronger MOF-guest interactions due to high quadruple moments of CO_2, and possible the interactions between CO_2 and free $-NH_2$ groups of the linkers. To investigate the porosity of both TMU-52 and TMU-25, we performed low-pressure N_2 and CO_2 adsorption measurements at 77 K and 195 K, respectively (Fig. 6). The materials showed CO_2/N_2 affinity and they exhibited a reversible type I isotherm, a characteristic of microporous materials, similar to most of the other sorbents. CO_2 is the most strongly adsorbed in TMU-25. This sorption behaviour can be attributed to the fact that the higher quadrupole moment and polarizablility of CO_2 molecules may induce better H-bonding interaction with the $-NH_2$ groups of L2 linker which are more accessible in TMU-25 channels with larger pillar.
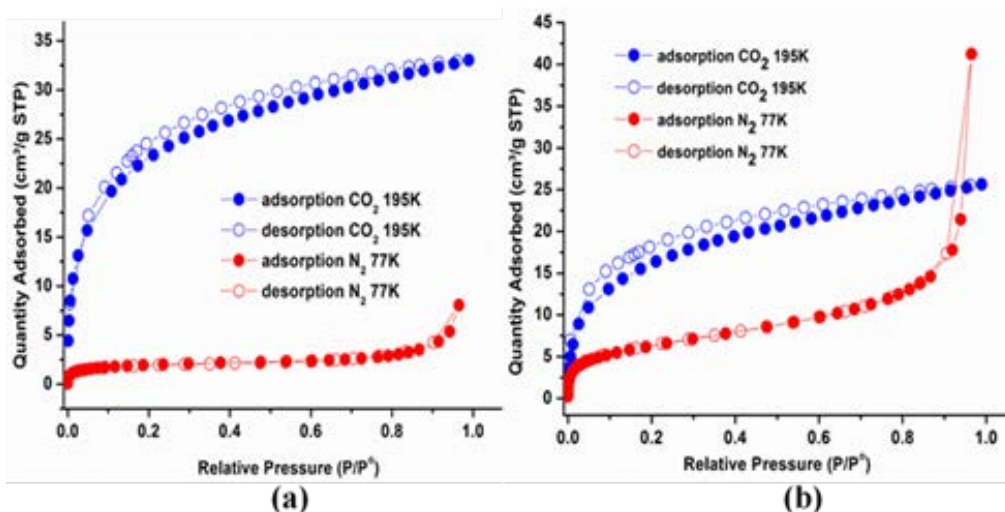
Figure 6. N_2 and CO_2 adsorption isotherms of TMU-25 (a) and TMU-52 (b) at 77 and 195 K, respectively.

Conclusion

In conclusion, herein we report a new two-fold interpenetrated pillar-layered MOF, (TMU-52), and studied structure-application relationship by using isoreticularity of this framework whit our recently reported TMU-25. Although these two MOFs possess the same SBUs and the same net topology, they show different catalyst selectivity and CO_2/N_2 affinity. In aldol-type condensation between malononitrile and α,β-unsaturated carbonyl compound, TMU-52 as a heterogeneous catalyst can act more selective than TMU-25, whiles the second one shows highly CO_2 adsorbing. The catalytic activity of these frameworks can arise from the basic functional groups on the linking struts, namely amine and imine groups. Superiority of TMU-52 in catalyst selectivity and more affinity of TMU-25 toward CO_2, can be related to the frameworks difference in aperture size and hydrophobicity. It has been indicated that a slight change in the MOF backbone could interestingly change the preference of the guests to be adsorbed or reacted while they have very little structure diversity.

Experimental *Section*

Synthesis of [Zn(NH₂-bdc)(L2)].2DMF (TMU-25) and [Zn(NH₂-bdc)(L1)].0.5DMF (TMU-52)

TMU-25 was synthesized according to the procedures described by us [21]. TMU-52 was synthesized according to the similar procedures of TMU-25. 1 mmol of $Zn(NO_3)_2.6H_2O$ (0.298 g), 0.5 mmol of L1 (0.143 g) and 1 mmol of NH_2-bdc (0.181 g) were first dissolved in 20 ml of N,N´-dimethylformamide (DMF). The mixture was then placed in a Teflon reactor and heated at 90 °C for 3 days. The mixture was then gradually cooled to room temperature during 48 hours. Brown crystals were formed on the walls of reactor with a 33% synthesis yield. Calculated elemental microanalysis data of synthesized TMU-52 (%): C: 57.82; H: 4.16; N: 11.56. Measured data (%): C: 57.75; H: 4.10; N: 11.48. m.p > 350° C, FT-IR data (KBr pellet, cm^{-1}): selected bands: 3470(w), 3359(w), 1669(vs), 1612(s), 1575 (vs), 1426(s), 1385 (vs), 1253(s), 1153(m), 1094 (m), 1016 (w), 836 (m) and 770(m), 633(m).

Crystallographic data: TMU-52: C27.5H22.5N5.5O4.5Zn, M= 567.38 g mol-1, Triclinic, P-1, a= 16.133(3) Å, b= 19.047(4) Å, c= 19.971(4) Å, α= 88.80(3)°, β= 81.75(3)°, γ= 89.94(3)°, V= 6072.0 (2) Å3, Z=8, ρcalc= 1.241 g cm-3, λ= 0.71073, T=100 K, R1= 0.0820, wR2= 0.2560, S= 1.070, CCDC number= 1856143.

Single-Crystal Diffraction

Crystals in viscous paraffin oil were mounted on cryoloops and intensity data were collected on the Australian Synchrotron MX1 beamline at 100 K with wavelength (λ = 0.71080 Å). The data were collected using the BlueIce [29] GUI and processed with the XDS [30] software package. The structures were solved by conventional methods and refined by full-matrix least-squares on all F2 data using SHELX-2014 in conjunction with the X-Seed [31] or Olex2 [32] graphical user interface. Anisotropic thermal parameters were refined for non-hydrogen atoms and hydrogen atoms were calculated and refined with a riding model. The crystals were twinned but these data were the best we could obtain and no more stable refinements can be achieved from the data.

Acknowledgments

References

[1]   a) W. Lu, Z. Wei, Z.-Y. Gu, T.-F. Liu, J. Park, J. Park, J. Tian, M. Zhang, Q. Zhang, T. Gentle Iii, M. Bosch, H.-C. Zhou, Chemical Society Reviews 2014, 43, 5561-5593; b) M. Li, D. Li, M. O'Keeffe, O. M. Yaghi, Chemical Reviews 2014, 114, 1343-1370.

[2]   H.-P. Xiao, A. Morsali, Helvetica Chimica Acta 2005, 88, 2543-2549.

[3]   L. Zhu, X.-Q. Liu, H.-L. Jiang, L.-B. Sun, Chemical Reviews 2017, 117, 8129-8176.

[4]   G. Li, H. Sun, H. Xu, X. Guo, D. Wu, The Journal of Physical Chemistry C 2017, 121, 26141-26154.

[5]   Y. Yang, P. Bai, X. Guo, Industrial & Engineering Chemistry Research 2017, 56, 14725-14753.

[6]   G. H. C. Prado, Y. Rao, A. de Klerk, Energy & Fuels 2017, 31, 14-36.

[7]   A. M. Shultz, A. A. Sarjeant, O. K. Farha, J. T. Hupp, S. T. Nguyen, Journal of the American Chemical Society 2011, 133, 13252-13255.

[8]   F. Zarekarizi, M. Joharian, A. Morsali, Journal of Materials Chemistry A 2018, 6, 19288-19329.

[9]   B.-Q. Ma, K. L. Mulfort, J. T. Hupp, Inorganic Chemistry 2005, 44, 4912-4914.

[10]   J. Seo, C. Bonneau, R. Matsuda, M. Takata, S. Kitagawa, Journal of the American Chemical Society 2011, 133, 9005-9013.

[11]   a) A. Azhdari Tehrani, H. Ghasempour, A. Morsali, G. Makhloufi, C. Janiak, Crystal Growth & Design 2015, 15, 5543-5547; b) A. A. Tehrani, S. Abedi, A. Morsali, J. Wang, P. C. Junk, Journal of Materials Chemistry A 2015, 3, 20408-20415.

[12]   S. Abedi, A. Azhdari Tehrani, H. Ghasempour, A. Morsali, New Journal of Chemistry 2016, 40, 6970-6976.

[13]   Y. Ding, X. Ni, M. Gu, S. Li, H. Huang, Y. Hu, Catalysis Communications 2015, 64, 101-104.

[14]   Y. Ogiwara, K. Takahashi, T. Kitazawa, N. Sakai, The Journal of Organic Chemistry 2015, 80, 3101-3110.

[15]   W. Fan, Y. Wang, Z. Xiao, L. Zhang, Y. Gong, F. Dai, R. Wang, D. Sun, Inorganic Chemistry 2017, 56, 13634-13637.

[16]   a) T. Truong, K. D. Nguyen, S. H. Doan, N. T. S. Phan, Applied Catalysis A: General 2016, 510, 27-33; b) V. Safarifard, S. Beheshti, A. Morsali, CrystEngComm 2015, 17, 1680-1685.

[17]   H. Yu, J. Xie, Y. Zhong, F. Zhang, W. Zhu, Catalysis Communications 2012, 29, 101-104.

[18]   J. M. Roberts, B. M. Fini, A. A. Sarjeant, O. K. Farha, J. T. Hupp, K. A. Scheidt, Journal of the American Chemical Society 2012, 134, 3334-3337.

[19]   O. M. Yaghi, M. O'Keeffe, N. W. Ockwig, H. K. Chae, M. Eddaoudi, J. Kim, Nature 2003, 423, 705.

[20]   M. Eddaoudi, J. Kim, N. Rosi, D. Vodak, J. Wachter, M. O'Keeffe, O. M. Yaghi, Science 2002, 295, 469-472.

[21]   H. Ghasempour, A. Azhdari Tehrani, A. Morsali, J. Wang, P. C. Junk, CrystEngComm 2016, 18, 2463-2468.

[22]   W. Xuan, C. Zhu, Y. Liu, Y. Cui, Chemical Society Reviews 2012, 41, 1677-1695.

[23]   a) V. Safarifard, S. Rodríguez-Hermida, V. Guillerm, I. Imaz, M. Bigdeli, A. Azhdari Tehrani, J. Juanhuix, A. Morsali, M. E. Casco, J. Silvestre-Albero, E. V. Ramos-Fernandez, D. Maspoch, Crystal Growth & Design 2016, 16, 6016-6023; b) J. Liu, P. K. Thallapally, B. P. McGrail, D. R. Brown, J. Liu, Chemical Society Reviews 2012, 41, 2308-2322.

[24]   M. Y. Masoomi, S. Beheshti, A. Morsali, Journal of Materials Chemistry A 2014, 2, 16863-16866.

[25]   AA Tehrani, H Abbasi, L Esrafili, A Morsali - Sensors and Actuators B 2018, 256, 706-710

[26]   V. A. Blatov, A. P. Shevchenko, V. N. Serezhkin, Journal of Applied Crystallography 2000, 33, 1193

[27]   A. Spek, Acta Crystallographica Section D 2009, 65, 148-155.

[28]   H. Ghasempour, A. Morsali, Polyhedron 2018, 151, 58-65.

[29]   T. M. McPhillips, S. E. McPhillips, H.-J. Chiu, A. E. Cohen, A. M. Deacon, P. J. Ellis, E. Garman, A. Gonzalez, N. K. Sauter, R. P. Phizackerley, S. M. Soltis, P. Kuhn, Journal of Synchrotron Radiation 2002, 9, 401-406.

[30]   K. W. Kabsch, Journal of Applied Crystallography 1993, 26, 795-800

[31]   L. J. Barbour, Journal of Supramolecular Chemistry 2001, 1, 189-191.

[32]   O. V. Dolomanov, L. J. Bourhis, R. J. Gildea, J. A. K. Howard and H. Puschmann, Journal of Applied Crystallography 2009, 42, 339-341.

Effects of pillaring linkers length on the size-dependent catalytic activity of two isoreticular metal–organic frameworks toward the aldol-type condensation reaction between malononitrile and α,β-unsaturated carbonyl compound. The result shows that the selectively of TMU-52 toward different substrate was significantly higher than TMU-25.

Effect of linker length in size-dependent catalytic activity of two IRMOFs

TMU-25   TMU-52